Journal of
MATERIALS RESEARCH

Tribological properties of fullerenes C_{60} and C_{70} microparticles

Wei Zhao,[a] Jinke Tang, and Ashok Puri
Department of Physics, University of New Orleans, New Orleans, Louisiana 70148

Ray L. Sweany
Department of Chemistry, University of New Orleans, New Orleans, Louisiana 70148

Yuxin Li and Liquan Chen
Institute of Physics, Chinese Academy of Sciences, P.O. Box 603, Beijing 100080, China

(Received 7 August 1995; accepted 6 June 1996)

The frictional behaviors of fullerenes C_{60} and C_{70} were studied because they were speculated to be solid lubricants. For the sublimated pure C_{60} films on Si(001), a high friction coefficient (0.55–0.8) was observed under different loads and pin materials. For the C_{70} film, the friction coefficient showed a pin dependence, which changed from 0.5 with an Al_2O_3 pin to about 0.9 with a 440 stainless steel pin. The relatively high friction coefficients of C_{60} and C_{70} films were due to the tendency of the C_{60} and C_{70} particles to clump and compress into high shear strength layers rather than due to the impurities in the fullerenes. The benzene-solvated $C_{60} \cdot 4C_6H_6$ and $C_{70} \cdot xC_6H_6$ showed a lowered friction coefficient (0.25 for $C_{60} \cdot 4C_6H_6$ and 0.3 for $C_{70} \cdot xC_6H_6$), which might result from the lowered shear strength of the hcp structure of $C_{60} \cdot 4C_6H_6$ and $C_{70} \cdot xC_6H_6$ molecular crystals in which the benzene molecules were intercalated.

I. INTRODUCTION

Since soccer-like fullerene C_{60} was discovered, its halogenated derivatives like $C_{60}F_{60}$ were speculated to be lubricants.[1] Later it was realized that unlike Teflon these fluorinated species were chemically unstable. Therefore, they failed to be lubricants.[2] For C_{60} pristine, its lubricating properties were anticipated because of its spherical shape, strong intramolecular and weak intermolecular bonding, and high chemical stability. It was expected to act as tiny ball bearings.[3,4] Pristine C_{60} solid is a molecular crystal which is of well-known face-centered cubic (fcc) structure at room temperature.[5] It can readily sublimate at temperatures about 450 °C in a vacuum, and dissolves in a wide range of nonpolar solvents such as benzene and hexane, which allows C_{60} molecules to easily attach to the surface of a substrate in the form of films. So far, the tribological properties of C_{60} were studied only by a few laboratories whose results showed some contradictions. Blau and Haberlin[3] reported a high friction coefficient (~0.6) of C_{60} powder with 90% purity (10% C_{70}) on aluminum. Bhattacharya *et al.*[6] obtained similar results for sublimed pure C_{60} film on Si_3N_4 substrate. In contrast, Bhushan *et al.*[4,7] found a low friction coefficient (~0.12) of sublimed C_{60} film on Si. They also observed an increased friction coefficient of C_{60} film as the amount of C_{70} and impurities in the film increased. We noticed that in their experiments, the measurement conditions including pin materials, loads, and sliding speed were not the same, which might influence their results. In addition, in Blau and Haberlin's work,[3] the coating of C_{60} particles on aluminum through evaporation of a drop of C_{60}-toluene solution showed a low friction coefficient characteristic of the substrates, which was explained to be due to the discontinuous deposition of microcrystals on the aluminum. To our knowledge, the evaporation of C_{60} solution results in solvated C_{60} microcrystals which consist of C_{60} and solvent molecules. The solvated C_{60} microcrystals have structures different from that of pristine C_{60} crystal.[8–11] Therefore, the solvated C_{60} crystals may show different frictional behaviors which are worthwhile to be explored further. For spheroidal fullerene C_{70}, it shows similar chemical and physical properties to those of C_{60}, and therefore it should pay the same role as C_{60} in lubricant application. However, at present no work regarding its tribological properties was done. In this paper, we discuss two areas of interest. First, we studied the frictional behavior of C_{60} and C_{70} films on Si(001) with different film thickness, pins, and loads. Second, we studied the frictional properties of benzene-solvated C_{60} and C_{70} microparticles on Si(001) and 304 stainless steel (304SS) disks under different loads and linear speeds with a pin-on-disk configuration in ambient air atmosphere at room temperature.

II. EXPERIMENTAL

Fullerenes C_{60} (purity $> 99.9\%$) and C_{70} (purity $> 98\%$) powders for film preparation were from the Department of Chemistry of Peking University. Their

[a]Author to whom correspondence should be addressed.

purity was examined by mass spectroscopy. The C_{60} and C_{70} thin films were grown by sublimating the pure C_{60} and C_{70} powders onto the (001) faced Si substrate in a vacuum of 10^{-5} Torr at about 400–600 °C. A pretreatment of powders in such a vacuum at about 350 °C for 40 min was carried out in order to drive off residual solvent left over from the purification process. The typical sublimating rate was 4 nm/min, i.e., about 5 molecular layers/min. The initial temperature of Si(001) substrate was kept at 300 K so that C_{60} and C_{70} can easily stick. After sublimating C_{60} and C_{70} for 5 min, the substrate temperature was raised to 400 K until the sublimation was done. The source-to-substrate distance was 2.5 cm. Two C_{60} films with thicknesses 1.2 (film A) and 3 μm (film B) and a C_{70} film of 0.7 μm thick were prepared for tribological study.

The 99.9% pure C_{60} powder for benzene-solvated C_{60} microparticle coating was from the Bucky USA Co. (Houston, TX). The coating of benzene containing C_{60} microparticles on Si(001) and 304SS disks was done by dropping a saturated solution of C_{60} in benzene on disks and subsequent evaporation of benzene. The composition of the evaporated microparticles has been reported to be $C_{60} \cdot 4C_6H_6$.[8] The particle distribution on disks was about 400 $\mu g/cm^2$ on Si(001) and 95 $\mu g/cm^2$ on 304SS, respectively. Similarly, a coating of benzene-solvated C_{70} microparticles ($C_{70} \cdot xC_6H_6$) on 304SS with distribution of 200 $\mu g/cm^2$ was obtained. At room temperature $C_{60} \cdot 4C_6H_6$ and $C_{70} \cdot xC_6H_6$ are stable, and benzene cannot be driven off even in vacuum. DSC measurements showed an endotherm between 200 and 300 °C for these benzene-solvated fullerenes, indicating that these benzene-fullerenes molecular crystals decomposed and the benzene molecules were driven off at that temperature region.

Knoop hardness measurements were performed on a Buehler microhardness tester at load 5 g. The time of applied load was 10 s.

The IR spectra of C_{60} and C_{70} were measured with a Perkin-Elmer 1760 Infrared Fourier Transform Spectrometer. The data were recorded by a Perkin-Elmer 7700 Professional Computer. A NaCl crystal was used as a substrate for benzene-solvated crystals.

A scanning electron microscope (SEM) was used to obtain topographic micrographs of C_{60} and C_{70} microparticles and the wear tracks.

The tribological measurements were carried out by using an ISC-200PC pin-on-disk tribometer (Implant Sciences Co.) which allows the tests with different loads and sliding speeds. The disk specimens of highly polished Si(001) were 1.0 × 1.0 cm large by 0.1 cm thick. Those of 304SS, 1.5 × 1.5 cm large by 0.5 cm thick, were mechanically polished to a surface roughness of less than 0.3 μm. The 3.2 mm diameter spheres of Al_2O_3 as well as 440 stainless steel (440SS) were used as pins. Pins were not coated and were highly polished. Applied loads ranged from 2.5 to 100 g. Friction coefficients were measured continuously, but only the steady state values reached near the end of 1000 cycles were plotted in the figures for comparison under different loads and sliding speeds. All data were collected by a PC computer.

III. RESULTS AND DISCUSSION

A. SEM micrographs, hardness, and IR spectra of films and solvated particles

The sublimated C_{60} films are polycrystalline, in which most of particles are of fcc structure, a few with a hcp phase. The detailed structure characterization can be found in our previous work.[12,13] The sublimated C_{70} film is primarily fcc with some admixture of a hcp phase.[14] The SEM micrographs of film A of C_{60} and the C_{70} film are shown in Fig. 1 in which the average sizes of C_{60} and C_{70} particles are about 0.57 and 0.26 μm, respectively. Knoop hardness data of the C_{60} films and the C_{70} film were obtained by a Buehler microhardness tester at load 5 g. The film A and film B of C_{60} exhibited a hardness of about 0.24 and 0.13 GPa, respectively, while the hardness of the C_{70} film was about 1.9 GPa. The data of the C_{60} films were close to those of Ossipyan *et al.*[15] who showed a Vickers microhardness of about 0.12–0.18 GPa for C_{60} crystal grown from solution. Gupta *et al.*[4] reported a hardness of about 1.2–2.0 GPa obtained by nanoindentation. They attributed the higher hardness of their C_{60} films to the beneficial effect in resisting deformation and/or cracking of C_{60} film, and partial contributions from

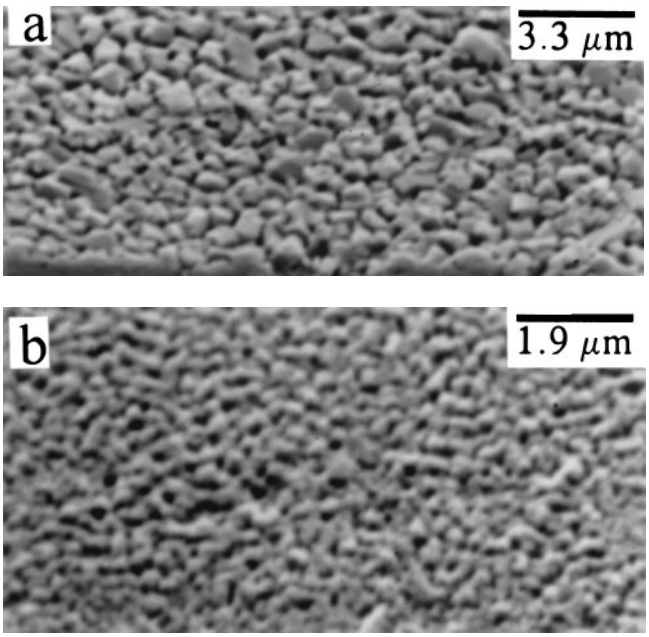

FIG. 1. SEM micrographs of the C_{60} film A (a) and the C_{70} film (b).

silicon substrate. In our case, the thinner C_{70} film showed a higher hardness than C_{60} film. The Si(001) substrate may give significant contributions to the hardness of this C_{70} film.

Figure 2 shows the SEM micrographs of $C_{60} \cdot 4C_6H_6$ microparticles on 304SS. Most of the particles were in the shape of a ball which was composed of petal-like microtwins. Their average size was about 5 μm. A few particles were flake-like crystals. On the other hand, for benzene-solvated C_{60} on Si(001) and benzene-solvated C_{70} on 304SS, most particles were flake-like crystals, which were typically seen in the samples crystallized from solution.

The IR spectra of C_{60} and C_{70} films as well as $C_{60} \cdot 4C_6H_6$ and $C_{70} \cdot xC_6H_6$ microparticles are shown in Fig. 3. In Fig. 3(a), for C_{60} film, there are only four lines at 526, 576, 1182, and 1428 cm^{-1}, suggesting C_{60} with high purity. For C_{70} film, several major lines locate at 535, 566, 578, 643, 675, 795, 1134, 1419, and 1431 cm^{-1}, which is consistent with the reported result of C_{70} film.[16] No lines from C_{60} were observed, indicating that the C_{70} film was free of C_{60} impurity. Figure 3(b) shows the IR spectra of the $C_{60} \cdot 4C_6H_6$ and $C_{70} \cdot xC_6H_6$ microparticles. For $C_{60} \cdot 4C_6H_6$, there are infrared (IR) lines of benzene at 671, 1034, 1460, and 1477 cm^{-1} in the as-prepared microparticles besides

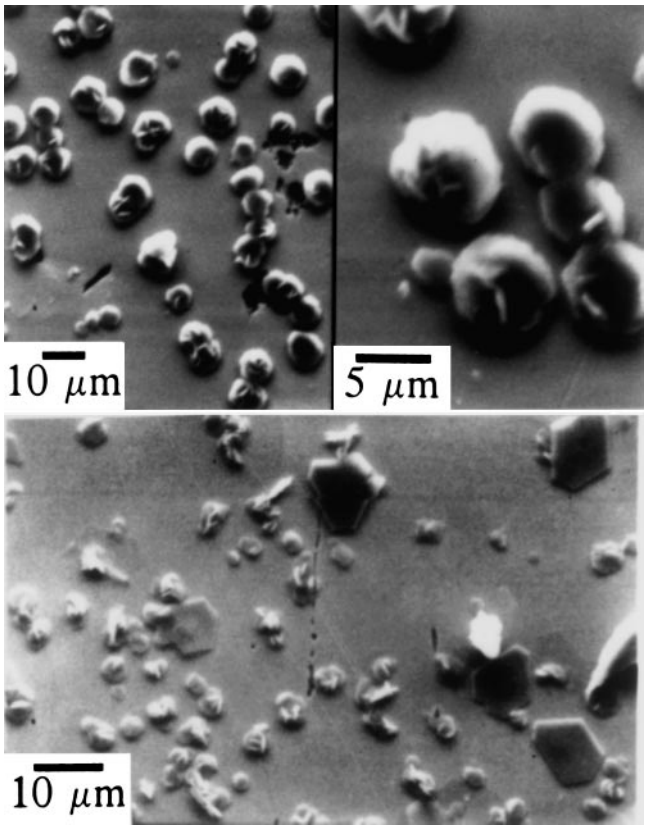

FIG. 2. SEM micrographs of $C_{60} \cdot 4C_6H_6$ microparticles on 304 stainless steel under different magnifications for selected areas.

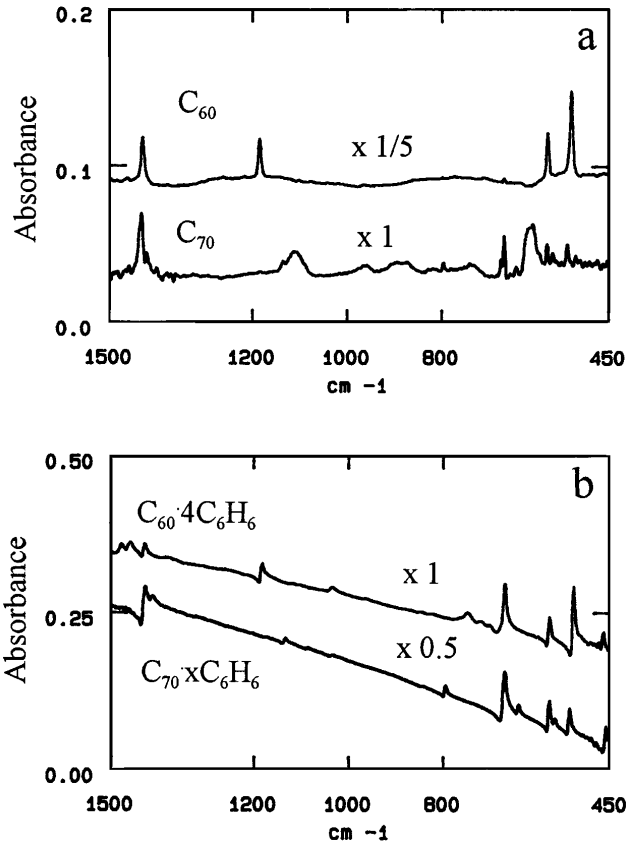

FIG. 3. Infrared spectra of the fullerenes. (a) C_{60} film B and C_{70} film. The broad bands in the spectrum of C_{70} film are from Si(001) substrate. This fact is further confirmed from the following spectrum of $C_{70} \cdot xC_6H_6$ in which those broad bands do not appear. (b) $C_{60} \cdot 4C_6H_6$ and $C_{70} \cdot xC_6H_6$ microparticles.

the four IR lines of pristine solid C_{60} at 526, 576, 1182, and 1428 cm^{-1},[17] in agreement with the fact that the as-prepared C_{60} microparticles are in the form of $C_{60} \cdot 4C_6H_6$,[8] which is of well-known hcp structure.[17] In the IR spectrum of $C_{70} \cdot xC_6H_6$, besides those lines of C_{70}, the line of benzene molecule at 671 cm^{-1} can be seen obviously, indicating the benzene molecules coexist in the crystals which also have the hcp structure.[14]

B. Frictional behaviors of C_{60} and C_{70} films under different loads and pin materials

Figure 4 shows the friction coefficients of disks Si(001), C_{60} film A and B, and the C_{70} film on Si(001) versus sliding distances. In Fig. 4(a), the load used was 2.5 g and an Al_2O_3 pin was used. The friction coefficient of Si(001) was about 0.65, and that of C_{60} film A was about 0.55. After 8 m of sliding distance, the friction coefficient of C_{60} film A reached the value of Si(001), indicating the film was broken through by the pin. The relatively high friction coefficient (0.55) was consistent with the results of Blau and Haberlin[3] and Bhattacharya *et al.*[6] This high friction coefficient of the

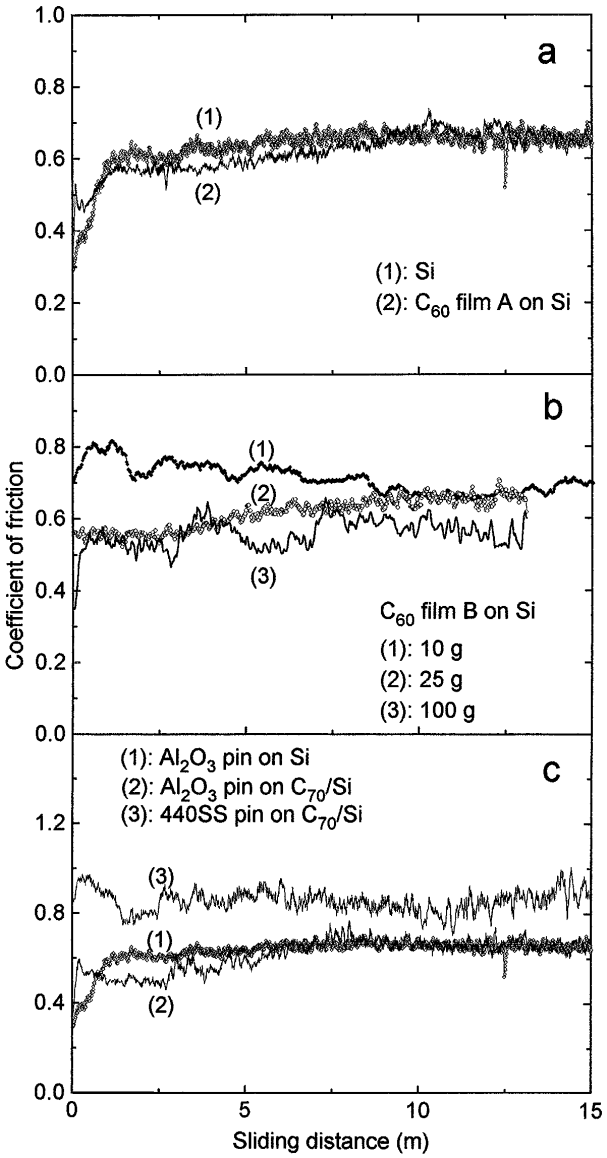

FIG. 4. Friction traces from Si(001) disks uncoated and coated with C_{60} film A and B, and C_{70} film under sliding speed 1.4 cm/s. (a) Si(001) and C_{60} film A with load 2.5 g and an Al_2O_3 pin. (b) C_{60} film B with different loads and an Al_2O_3 pin. (c) C_{70} film with different pins and 2.5 g load.

C_{60} film was not caused by the impurity of C_{60} because the C_{60} powder used here is >99.9% pure as confirmed by mass spectrometer and IR. For further investigation of C_{60} tribological properties, we used a thicker film, film B, to measure its friction coefficient under different loads.

The friction coefficient of C_{60} film B under different loads, as a function of sliding distance, is shown in Fig. 4(b). Under 10 g load, the friction coefficient of the film B reached about 0.8 at the first several meters of sliding distance, and then gradually reduced to 0.7 at the following sliding distance. With 25 g load, the friction coefficient changed from 0.55 at the beginning to 0.7 at the end. With a heavier load of 100 g, the frictional behavior was quite fluctuating compared to lighter loads. The coefficient of friction was about 0.55.

The difference of the friction coefficient in Films A and B may result from the different crystallinities and defect densities in both films.[12,13] Further experiments using high resolution electron microscope to study the structure of those worn films are being performed.

The possible effect of different pin materials on the frictional behaviors of C_{60} was evaluated too. A different pin, 440SS pin, was used for film A, and similar frictional behavior was observed.

Gupta *et al.* have found that the presence of C_{70} and other impurities increases the friction coefficient of C_{60} films.[4] However, the frictional properties of C_{70} itself were unclear and not investigated. Figure 4(c) shows the friction coefficient of the C_{70} film versus sliding distance with two types of pins. The load was 2.5 g. With an Al_2O_3 pin, the film showed a friction coefficient of about 0.5 before its friction coefficient reached the value of the substrate Si(001). However, a much higher friction coefficient (0.9–1.0) of the C_{70} film was observed with a 440SS pin. Subsequently, we will discuss the origin of this high friction coefficient of the C_{70} film with reference to the results of SEM.

As seen from the above results, a high friction coefficient (0.55–0.8) for C_{60} films was observed which was not due to the impurity of C_{60}. Changing loads and pin materials could not obviously reduce their friction coefficient. For the C_{70} film, the friction coefficient showed a pin dependence, which changed from 0.5 with an Al_2O_3 pin to about 0.9 with a 440SS pin. The relatively high friction coefficients of C_{60} and C_{70} films were due to the tendency of the C_{60} and C_{70} particles to clump and compress into a high shear strength layer which was hard to deform, as shown in Fig. 5 and Fig. 6.

C. SEM micrographs of wear tracks of C_{60} and C_{70} films

Figure 5 shows the SEM micrographs of the wear track of film A of C_{60} after the sliding distance shown in Fig. 4(a). The film on the track was ploughed up by the pin [Fig. 5(a)] and the particles on the track were compressed into patches of smooth denser layers [Fig. 5(b)]. We also observed that a tenacious transfer film was formed on the pin surface which separated the pin and the disk. This kind of transfer film can be clearly seen in Fig. 6. In Fig. 6, the wear track of the C_{70} film and the surface of the 440SS pin after the sliding distance shown in Fig. 4(c) were presented. Similarly, the film on wear track was worn out because of ploughing by the 440SS pin during sliding [Fig. 6(a)]. On the mating surface of the 440SS pin, a dark-appearing tenacious transfer film with denser density was formed [Figs. 6(b)

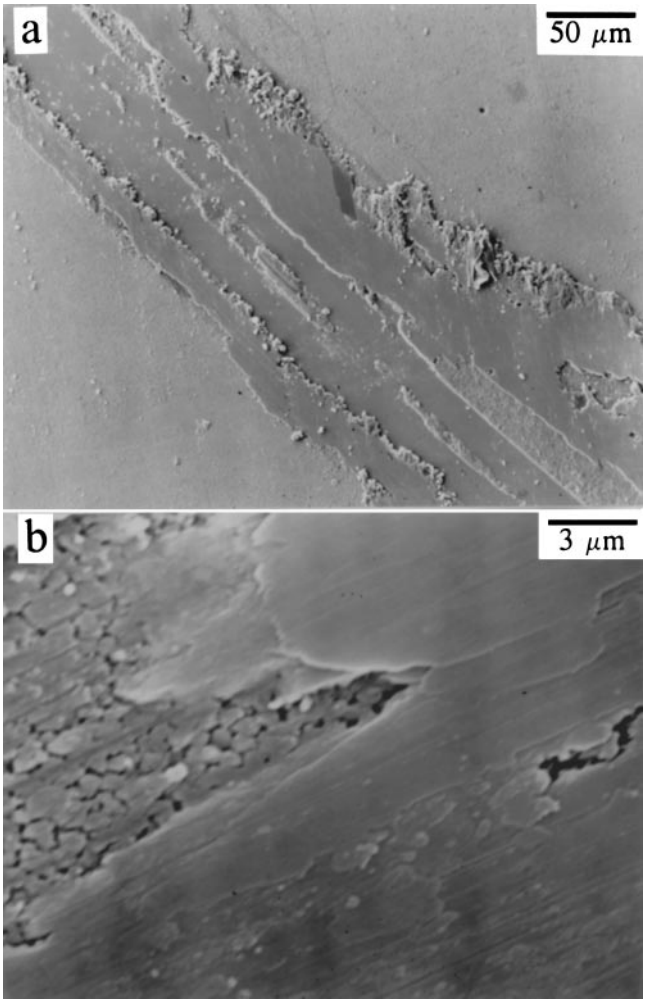

FIG. 5. SEM micrographs of (a) the worn C_{60} film A on Si(001) and (b) the patch of the compact of C_{60} film on the track.

and 6(c)]. The shear strength of this dense, dark transfer film resulted in significant surface traction during sliding. Consequently, high friction coefficients were observed for the 440SS pin on the disk. These results agreed with those of Blau and Haberlin.[3]

D. Lowered friction coefficients of benzene-solvated C_{60} and C_{70} particles

In contrast to the pure C_{60} and C_{70} films, the benzene-solvated C_{60} and C_{70} particles show lowered friction coefficients. Figure 7(a) shows the friction coefficients of the Si(001) disks uncoated and coated with $C_{60} \cdot 4C_6H_6$ versus sliding distances. The loads were 10 g. The friction coefficient of uncoated Si(001) increased at the beginning, and it reached the maximum ($\sim$0.65) near 3 m of sliding distance. The friction coefficient of $C_{60} \cdot 4C_6H_6$-coated Si(001) showed a lowered value $\sim$0.35 before it reached the value of Si(001). The lowered friction coefficient of 304SS by coating of benzene-solvated C_{60} and C_{70} particles was quite

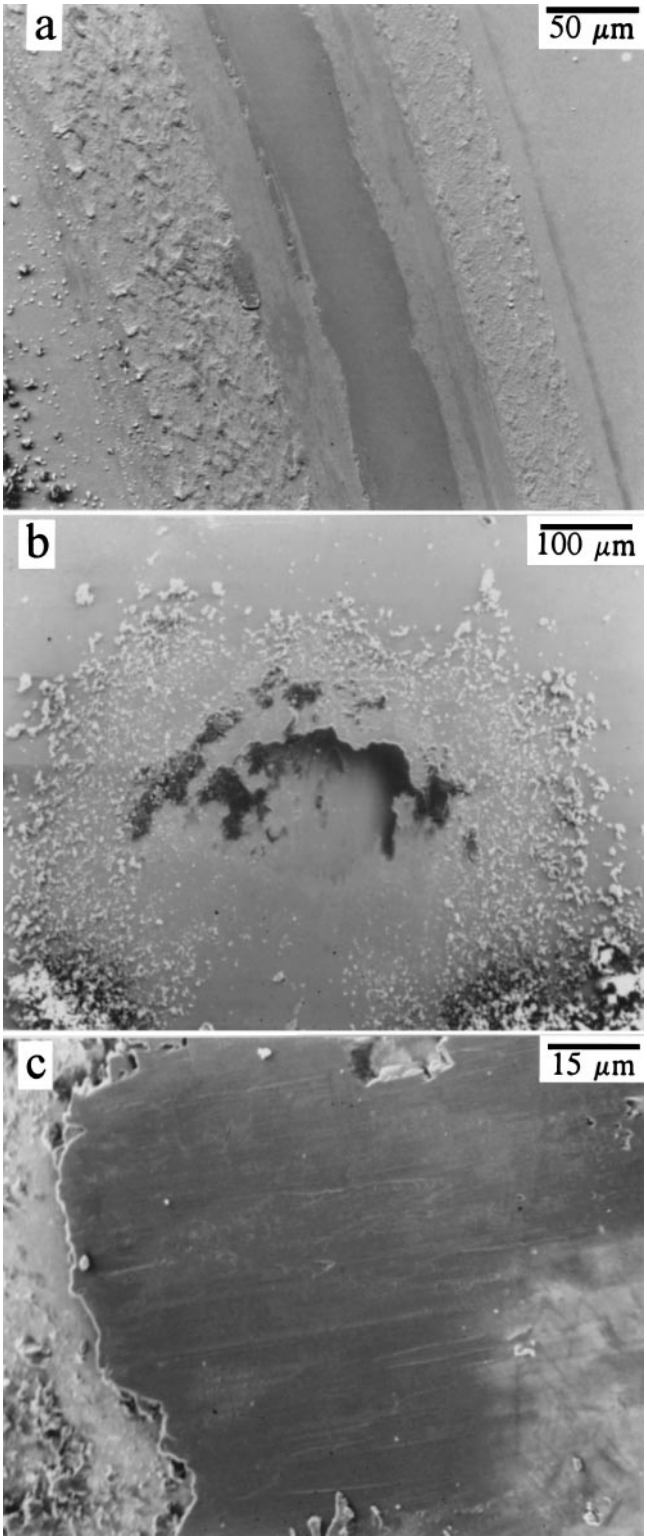

FIG. 6. SEM micrographs of (a) the worn C_{70} film on Si(001) and (b, c) the 440SS pin surface with patches of the compact of C_{70} film under different magnifications.

evident in Fig. 7(b). The loads used were 25 g. The friction coefficient of uncoated 304SS was $\sim$0.8. For $C_{60} \cdot 4C_6H_6$-coated 304SS, it has a lowered friction co-

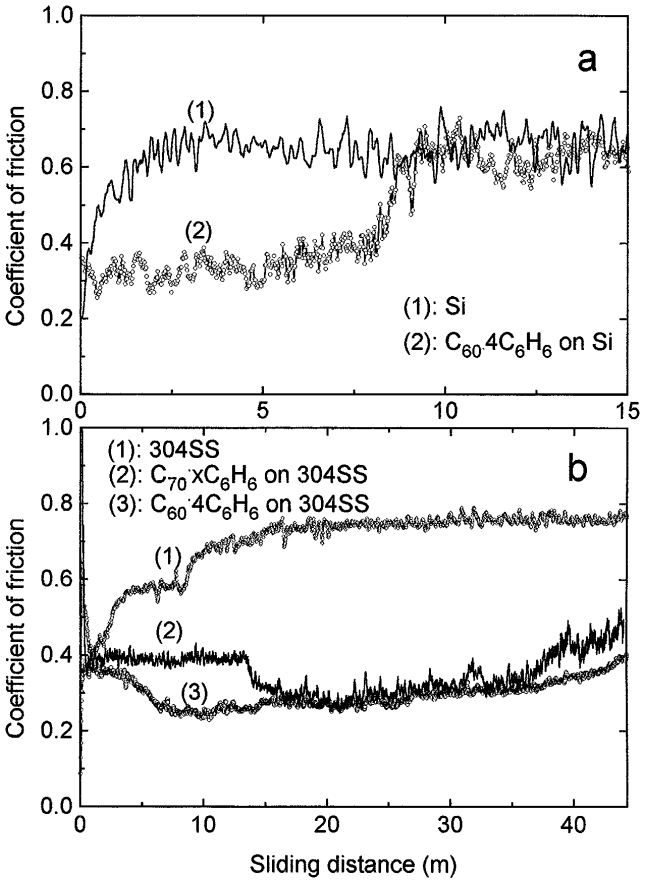

FIG. 7. Friction traces from Si(001) (a) and 304SS (b) disks uncoated and coated with $C_{60} \cdot 4C_6H_6$ and $C_{70} \cdot xC_6H_6$ under sliding speed 2 cm/s. An Al_2O_3 pin was used. (a) Si(001) and $C_{60} \cdot 4C_6H_6$ with load 10 g. (b) 304SS, $C_{60} \cdot 4C_6H_6$, and $C_{70} \cdot xC_6H_6$ with 25 g load.

efficient of 0.35 at the beginning. After near 6 m sliding distance, its value further reduced to 0.25. The reduction of friction coefficient during sliding suggested that a lubricating layer was forming between the pin and the disk. Similarly, for $C_{70} \cdot xC_6H_6$-coated 304SS, it had a friction coefficient of 0.4 at the first several sliding distances, and then its value reduced to 0.3 after 15 m sliding distance. The optical micrographs of the wear tracks showed that much less wear occurred on the $C_{60} \cdot 4C_6H_6$-coated 304SS then the uncoated 304SS, and these reductions were accompanied by a change from an adhesive wear mode to an abrasive wear mode.[18] The above results indicated that the coating of $C_{60} \cdot 4C_6H_6$ and $C_{70} \cdot xC_6H_6$ on 304SS reduced friction as well as wear. The friction coefficients ($\sim$0.25 for $C_{60} \cdot 4C_6H_6$ coating and 0.3 for $C_{70} \cdot xC_6H_6$ coating) were reduced by $\sim$70% in comparison to uncoated values ($\sim$0.8). We noticed that these benzene-solvated fullerenes are chemically stable at room temperature. After being exposed to air for half a year, the steels coated with $C_{60} \cdot 4C_6H_6$ and $C_{70} \cdot xC_6H_6$ particles still show lowered coefficients of friction.

The load and sliding speed dependences of the friction coefficients of 304SS disks uncoated and coated with $C_{60} \cdot 4C_6H_6$ are shown in Fig. 8. All samples showed less change upon different linear speeds. Under different loads, the friction coefficients of the uncoated 304SS disk were almost the same ($\sim$0.75). For the $C_{60} \cdot 4C_6H_6$-coated 304SS disk, its friction coefficient was about 0.44 at 5 g load. Upon increasing loads, the friction coefficients of $C_{60} \cdot 4C_6H_6$-coated disks showed a minimum value of 0.25 at 25 g load before it reached the uncoated values beyond 50 g load. The low coefficient of friction observed at lighter loads represents a reduction of 50–70% in comparison to the uncoated value due to the presence of $C_{60} \cdot 4C_6H_6$ coating. Similar results were also observed on 304SS coated with solvated C_{70} microparticles.

The relatively high friction coefficient of benzene-free C_{60} particles layer is due to the tendency of the C_{60} particles to clump and compress into a high shear

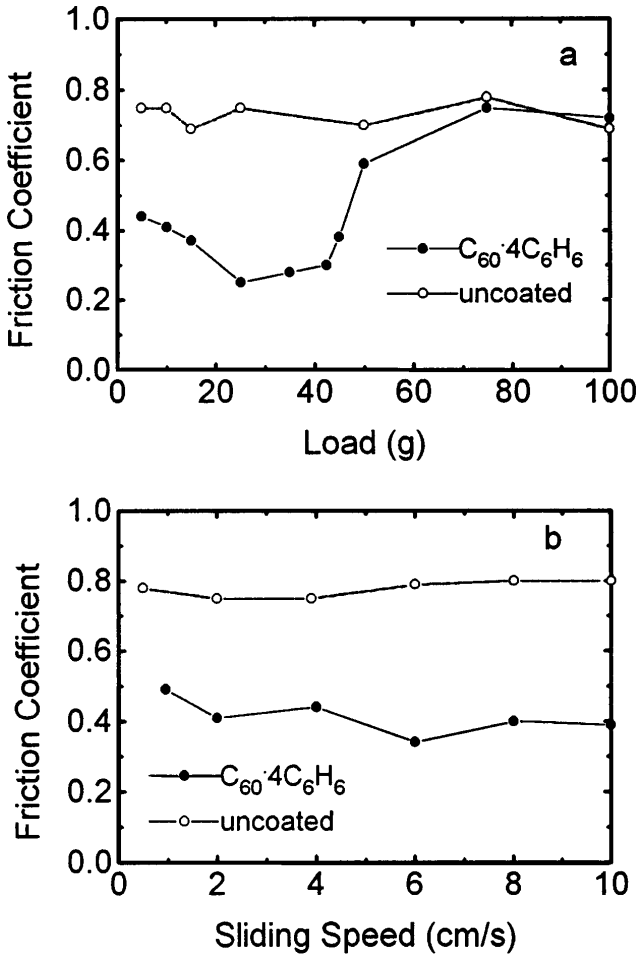

FIG. 8. Friction coefficient at the end of 1000 cycle pin-on-disk test of 304 stainless steel disks uncoated and coated with $C_{60} \cdot 4C_6H_6$, plotted as functions of load (a) (2 cm/s sliding speed) and sliding speed (b) (10 g load). Al_2O_3 pins were used.

strength layer. Instead, in the case of solvated C_{60} and C_{70} microparticles layer, their reduced friction may be related to their preferred structure which prevents the formation of the high shear strength layer.

The solvated C_{60} and C_{70} crystals have shown different structures from solvent-free fullerene crystals because of the incorporation of guest molecules into the host C_{60} and C_{70}. For example, C_{60} crystals grown from benzene,[8,19] *n*-heptane,[20] CCl_4,[21] and a benzene solution containing CH_2I_2[22] have a hexagonal structure.[17] C_{60} crystals grown from CS_2[23] or *n*-pentane[24] in an untwinned form show an orthorhombic lattice. C_{60} crystals with cyclohexane crystallize in the cubic system.[10] The common feature in the structures of these crystals is that the spherical C_{60} molecules are close-packed with the insertion of the solvent molecules. A representative structure of these solvated crystals is the hexagonal close-packed $C_{60} \cdot 4C_6H_6$, as shown in Fig. 9. In this figure, the $C_{60} \cdot 4C_6H_6$ crystal can be visualized in terms of a hexagonal close-packed arrangement of C_{60} molecules with the hexagonal axil along *a*. The C_{60} spheres within a close-packed layer are then moved well apart and the benzene molecules are inserted, and the close-packed layers moved toward each other along the *a*-axis until adjacent molecules (along the *a*-axis) touch. Three of the four benzene rings lie parallel to the C_{60} molecular surface, and the other appears to fill an interstice between the other molecules.[8] A stereoview of the hcp structure of solvated C_{60} crystals can also be found in Refs. 19 and 22. Similarly, $C_{70} \cdot xC_6H_6$ also has a hcp structure.[14] Therefore, the intercalation of the benzene molecules into the close-packed layers may produce a low shear strength for $C_{60} \cdot 4C_6H_6$ as well as for $C_{70} \cdot xC_6H_6$, which makes C_{60} and C_{70} molecules act like tiny ball bearings working at the interface.

The coatings on 304SS disks using solvated C_{60} with different solvents, toluene, CS_2, and CCl_4, etc. indicate that these solvated C_{60} microparticles also lower the friction coefficient of 304SS as do the benzene-solvated fullerenes.[25] Because $C_{60} \cdot xCS_2$ crystals have an orthorhombic structure, these results indicate that the hcp structure of solvated C_{60} crystals may not be the only preferred structure in lowering the friction. Furthermore, these preliminary results suggest that the intercalated solvent molecules may have a twofold function in lowering the friction coefficient; i.e., they may prevent the formation of the high shear strength layer as occurred in pure fullerene thin film, and make C_{60} and C_{70} molecules act like interface ball bearings. The structure characterization of the lubricating layer of these solvated fullerenes formed during sliding is under way.

IV. CONCLUSIONS

The above results exhibited a high friction coefficient (0.55–0.8) for C_{60} films on which the purity of C_{60}, loads, and pin materials have no bearing. For the C_{70} film, the friction coefficient showed pin dependence, which changed from 0.5 with Al_2O_3 pin to about 0.9 with 440SS pin. The relatively high friction coefficients of C_{60} and C_{70} films were due to the tendency of the C_{60} and C_{70} particles to clump and compress into high shear strength layers which were hard to deform. The coating of $C_{60} \cdot 4C_6H_6$ and $C_{70} \cdot xC_6H_6$ on 304SS reduced friction as well as wear. The friction coefficients (0.25 for $C_{60} \cdot 4C_6H_6$ coating and 0.3 for $C_{70} \cdot xC_6H_6$ coating at 25 g loads) were reduced by ~70% in comparison to uncoated values (~0.8). In the case of solvated C_{60} and C_{70} microparticle layers, the benzene molecules were intercalated into the C_{60} and C_{70} lattice, which may play the role of a molecular lubricant among C_{60} ball molecules, and the C_{60} and C_{70} molecules acted like tiny ball bearings at the interface.

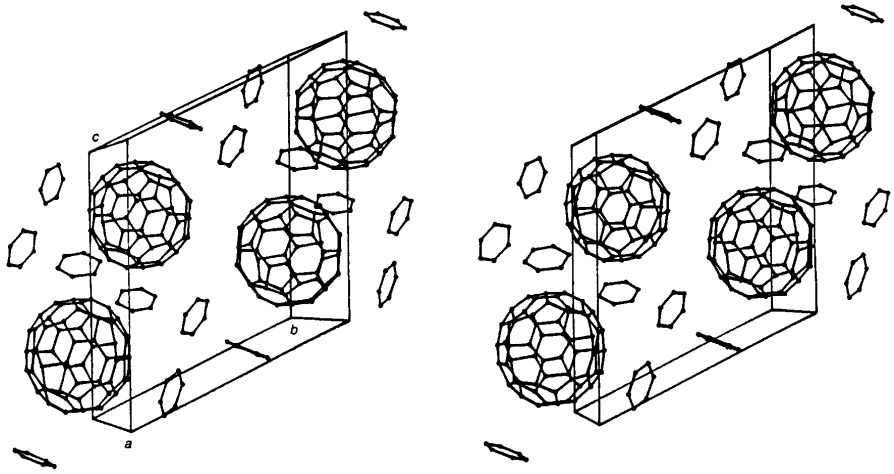

FIG. 9. Stereopair showing the crystal packing for $C_{60} \cdot 4C_6H_6$ with lattice parameters $a = 9.961(3)$, $b = 15.072(7)$, and $c = 17.502(5)$ Å, reproduced with permission from Ref. 8.

Our results suggest that pure (undoped) fullerenes C_{60} and C_{70} are not particularly lubricous under ambient conditions. However, benzene-solvate can be adopted to modify the crystal structure of the fullerenes in order for them to form a preferred structure with low shear strength. Benzene-solvated fullerenes are stable in the air, and the benzene molecules cannot be driven out until above 200 °C. The steels coated with solvated fullerenes still show low friction coefficient after keeping them in the air for half a year. These results suggest that the solvated fullerenes may have potential applications as lubricants. They are also good precursors for the investigation of tribological mechanism at nanoscale because these fullerenes possess the unique properties of a sphere of diameter in nanometers.

ACKNOWLEDGMENTS

This work was supported by the U.S. Department of Energy, Louisiana Education Quality Support Fund and Research Corporation. The authors thank Dr. David R. M. Walton and his co-authors, and the Royal Society of Chemistry for permission to use Fig. 1 of Ref. 8.

REFERENCES

1. H. W. Kroto, J. R. Heath, S. C. O'Brien, R. F. Curl, and R. E. Smalley, Nature (London) **318**, 162 (1985).
2. R. Taylor, A. G. Avent, T. J. Dennis, J. P. Hare, H. W. Kroto, D. R. M. Walton, J. H. Holloway, E. G. Hope, and G. J. Langley, Nature (London) **355**, 27 (1992).
3. P. J. Blau and C. E. Haberlin, Thin Solid Films **219**, 129 (1992).
4. B. K. Gupta, B. Bhushan, C. Capp, and J. V. Coe, J. Mater. Res. **9**, 2823 (1994).
5. P. A. Heiney, J. E. Fischer, A. R. McGhie, W. J. Romanow, A. M. Denenstein, J. P. McCauley, and A. B. Smith III, Phys. Rev. Lett. **66**, 2911 (1991).
6. R. S. Bhattacharya, A. K. Rai, J. S. Zabinski, and N. T. McDevitt, J. Mater. Res. **9**, 1615 (1994).
7. B. Bhushan, B. K. Gupta, G. W. Van Cleef, C. Capp, and J. V. Coe, Appl. Phys. Lett. **62**, 3253 (1993).
8. M. F. Meidine, P. B. Hitchcock, H. W. Kroto, R. Taylor, and D. R. M. Walton, J. Chem. Soc., Chem. Commun., 1534 (1992).
9. R. M. Fleming, A. R. Kortan, B. Hessen, T. Siegrist, F. A. Thiel, P. Marsh, R. C. Haddon, R. Tycko, G. Dabbagh, M. L. Kaplan, and A. M. Mujsce, Phys. Rev. B **44**, 888 (1991).
10. S. M. Gorun, K. M. Creegan, R. D. Sherwood, D. M. Cox, V. W. Day, C. S. Day, R. M. Upton, and C. E. Briant, J. Chem. Soc., Chem. Commun., 1556 (1991).
11. X. D. Shi, A. R. Kortan, J. M. Williams, A. M. Kini, B. M. Savall, and P. M. Chaikin, Phys. Rev. Lett. **68**, 827 (1992).
12. W. Zhao, W. L. Zhou, L. Q. Chen, Y. Z. Huang, Z. B. Zhang, K. K. Fung, and Z. X. Zhao, J. Solid State Chem. **112**, 412 (1994).
13. W. L. Zhou, W. Zhao, K. K. Fung, L. Q. Chen, and Z. B. Zhang, Physica C **214**, 19 (1993).
14. G. B. M. Vaughan, P. A. Heiney, J. E. Fischer, D. E. Luzzi, D. A. Ricketts-Foot, A. R. McGhie, Y. W. Hui, A. L. Smith, D. E. Cox, W. J. Romanow, B. H. Allen, N. Coustel, J. P. McCauley, Jr., and A. B. Smith III, Science **254**, 1350 (1991).
15. Yu. A. Ossipyan, V. S. Bobrov, Yu. S. Grushko, R. A. Dilanyan, O. V. Zharikov, M. A. Lebyodkin, and V. Sh. Sheckhtman, Appl. Phys. A **56**, 413 (1993).
16. B. Chase, N. Herron, and E. Holler, J. Phys. Chem. **96**, 4262 (1992).
17. W. Krätschmer, L. D. Lamb, K. Fostiropoulos, and D. R. Huffman, Nature (London) **347**, 354 (1990).
18. W. Zhao, J. Tang, A. Puri, A. U. Falster, and W. B. Simmons, Jr., in *Mechanical Behavior of Diamond and Other Forms of Carbon,* edited by M. D. Drory, M. S. Donley, D. Bogy, and J. E. Field (Mater. Res. Soc. Symp. Proc. **383**, Pittsburgh, PA, 1995), p. 313.
19. A. L. Balch, J. W. Lee, B. C. Noll, and M. M. Olmstead, J. Chem. Soc., Chem. Commun., 56 (1993).
20. R. Ceolin, V. Agafonov, B. Bachet, A. Gonthier-Vassal, H. Szwarc, S. Toscani, G. Keller, C. Fabre, and A. Rassat, Chem. Phys. Lett. **244**, 100 (1995).
21. R. Ceolin, V. Agafonov, D. Andre, A. Dworkin, H. Szwarc, J. Dugue, B. Keita, L. Nadjo, C. Fabre, and A. Rassat, Chem. Phys. Lett. **208**, 259 (1993).
22. U. Geiser, S. K. Kumar, B. M. Savall, S. S. Harried, K. D. Carlson, P. R. Mobley, H. H. Wang, J. M. Williams, R. E. Botto, W. Liang, and M.-H. Whangbo, Chem. Mater. **4**, 1077 (1992).
23. K. Kikuchi, S. Suzuki, K. Saito, H. Shiromaru, A. A. Zakhidov, A. Ugawa, K. Imaeda, H. Inokuchi, and K. Yakushi, Physica C **185–189**, 415 (1991).
24. S. Pekker, G. Faigel, K. Fodor-Csorba, L. Granasy, E. Jakab, and M. Tegze, Solid State Commun. **83**, 423 (1992).
25. W. Zhao, J. Tang, C. J. O'Connor, and C. E. O'Connor, unpublished.